



# Trivalent chromium isotopes in the eastern tropical North Pacific oxygen-deficient zone

Tianyi Huang<sup>a,b</sup>, Simone B. Moos<sup>a,b</sup>, and Edward A. Boyle<sup>a,1</sup>

<sup>a</sup>Department of Earth, Atmospheric, and Planetary Sciences, Massachusetts Institute of Technology, Cambridge, MA 02139; and <sup>b</sup>Massachusetts Institute of Technology/Woods Hole Oceanographic Institution Joint Program in Oceanography, Cambridge, MA 02139

Contributed by Edward A. Boyle, November 19, 2020 (sent for review October 24, 2019; reviewed by Chris Holmden and Samuel L. Jaccard)

**Changes in chromium (Cr) isotope ratios due to fractionation between trivalent [Cr(III)] and hexavalent [Cr(VI)] are being utilized by geologists to infer oxygen conditions in past environments. However, there is little information available on Cr in the modern ocean to ground-truth these inferences. Transformations between the two chromium species are important processes in oceanic Cr cycling. Here we present profiles of hexavalent and trivalent Cr concentrations and stable isotope ratios from the eastern tropical North Pacific (ETNP) oxygen-deficient zone (ODZ) which support theoretical and experimental studies that predict that lighter Cr is preferentially reduced in low-oxygen environments and that residual dissolved Cr becomes heavier due to removal of particle-reactive Cr(III) on sinking particles. The Cr(III) maximum dominantly occurs in the upper portion of the ODZ, implying that microbial activity (dependent on the sinking flux of organic matter) may be the dominant mechanism for this transformation, rather than a simple inorganic chemical conversion between the species depending on the redox potential.**

chromium isotopes | oxygen-deficient zones | trace elements | trivalent chromium | hexavalent chromium

Chromium is a trace metal dominantly present in its thermodynamically stable hexavalent form—chromate ( $\text{CrO}_4^{2-}$ ) or bichromate ( $\text{HCrO}_4^-$ )—in most of the oxygenated ocean (1–3). Previous work on Cr concentrations in the ocean shows that it is somewhat depleted in the surface ocean and enriched in deep waters with a concentration increase from the deep Atlantic to the deep Pacific Ocean (1). It is generally assumed that this distribution is the result of biological uptake of Cr in the euphotic zone and regeneration from sinking particles. In oxic waters a small fraction exists as reduced trivalent form due to photochemistry or biological activity (4) and slow oxidation kinetics. When the oxygen level is extremely low ( $<2 \mu\text{mol/kg}$ ), Cr(III) becomes the thermodynamically favored species, and high levels of Cr(III) have been observed in oxygen-deficient zones (ODZs) (5). The kinetics of inorganic thermodynamic Cr reduction are slow, and it appears that microbial activity or reducing agents such as ferrous ion, sulfide, and hydrogen peroxide may be responsible for the Cr(III) levels seen in low-oxygen environments (rather than a simple thermodynamic response of Cr to the redox conditions). These transformations between Cr species are important processes in global Cr cycling. As the deoxygenation of the ocean expands in the modern global ocean (6, 7) or may have occurred in certain periods of the earth's history (8, 9), Cr(VI) can potentially be reduced in larger regions to a greater extent than today.

Cr stable isotope ratios are a new tool that has been developed during the past decade to study Cr redox cycling. By convention, Cr isotopes are reported in delta notation:

$$\delta^{53}\text{Cr}(\text{‰}) = \left( \frac{(^{53}\text{Cr}/^{52}\text{Cr})_{\text{sample}}}{(^{53}\text{Cr}/^{52}\text{Cr})_{\text{standard}}} - 1 \right) \times 1,000,$$

where the standard used is Cr standard reference material 979. Although there are very few data available, oceanic Cr isotope ratios are heavier in the upper ocean than deeper waters, presumably as a result of fractionation during biological uptake (10–13). It is also likely that the Cr(III) produced in ODZs has low  $\delta^{53}\text{Cr}$ , although there are very few data as of yet (ref. 14, whose data significantly differ from ours). This hypothesis derives from theoretical thermodynamic and laboratory experimental studies which indicate the preferential reduction of isotopically light Cr(III) from Cr(VI) (15–19).

Most of the available oceanic Cr isotope data are from the oxic ocean and follow a linear global  $\delta^{53}\text{Cr}\text{-log}[\text{Cr}]$  relationship, as if there were Rayleigh fractionation from the deep ocean Cr as it is progressively removed by biological activity in the euphotic zone. The total dissolved Cr isotope data from the Peruvian ODZ also largely fits into this global relationship, suggesting that Cr cycling as expressed by total dissolved Cr in the Peruvian ODZ is in line with the global picture (20). In this study, we report Cr isotopes for Cr(III), Cr(VI), and total Cr from three stations within the eastern tropical North Pacific (ETNP) ODZ (ETNP ODZ; Figs. 1 and 2). Two of these (P1 and P2) were collected on cruises *Roger Revelle* 1804-5 (April to May 2018) and KM1920 (September 2019). The third (2T) was collected on cruise *New Horizon* 1410 (May 2014) whose primary data are reported in ref. 21. This dataset will disentangle some interspecies Cr processes, which are included within the total dissolved Cr data.

To separate Cr species and analyze their isotopic compositions, we used a  $\text{Mg}(\text{OH})_2$  coprecipitation method similar to that

## Significance

Chromium isotopes have been used to study ancient earth atmospheric oxygen levels and seem promising as a paleoredox proxy. However, few studies have focused on its cycling in the modern ocean. Here we analyzed samples from oxygen-deficient zones and investigated how chromium speciation and isotopes respond to extremely low oxygen environments, which helps to unravel the chromium redox cycling and the associated isotopic fractionation. The isotopic composition of trivalent chromium in the eastern tropical North Pacific oxygen-deficient zones is lighter than total dissolved chromium and residual hexavalent chromium. This finding supports the preferential reduction of isotopically light Cr found in theoretical and experimental studies and is fundamental to the usage of Cr isotopes as a paleoredox proxy.

Author contributions: T.H., S.B.M., and E.A.B. designed research; T.H. and S.B.M. performed research; E.A.B. contributed new reagents/analytic tools; T.H. and E.A.B. analyzed data; and T.H., S.B.M., and E.A.B. wrote the paper.

Reviewers: C.H., University of Saskatchewan; and S.L.J., University of Lausanne.

The authors declare no competing interest.

Published under the PNAS license.

<sup>1</sup>To whom correspondence may be addressed. Email: eaboyle@mit.edu.

This article contains supporting information online at <https://www.pnas.org/lookup/suppl/doi:10.1073/pnas.1918605118/-DCSupplemental>.

Published February 18, 2021.

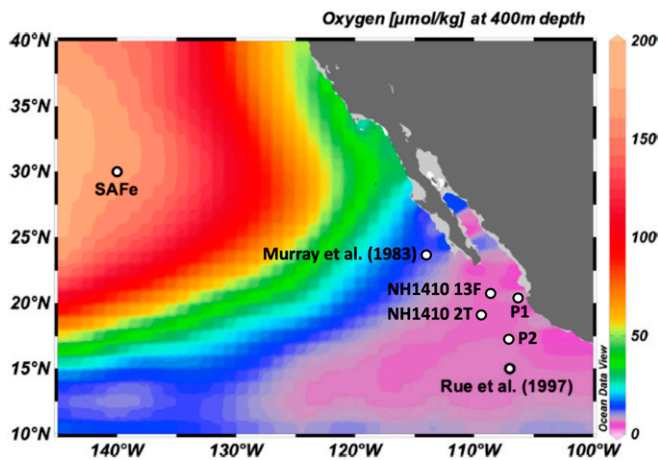


Fig. 1. Sampling sites (P1 and P2) and nearby stations (13F, 2T, and ref. 5). Reprinted from ref. 21. Copyright (2020), with permission from Elsevier.

reported in refs. 12, 22 with some differences in the details: 1) A  $^{50}\text{Cr}$ - $^{54}\text{Cr}$  double spike was added to each sample before collecting  $\text{Mg}(\text{OH})_2$ . The double-spike was allowed to equilibrate with samples for  $\sim 6$  h. Tests of equilibration time between 0.5 and 12 h show no difference in isotopic values (*SI Appendix, Fig. S2*). 2) No iron coprecipitation was done to separate Cr(III) from the Mg matrix. The  $\text{Mg}(\text{OH})_2$  pellets were dissolved in HCl, pH-adjusted and ready for column chromatography as described in ref. 11. 3) To determine Cr(VI) isotopic composition, we filtered the supernatant after the  $\text{Mg}(\text{OH})_2$  coprecipitation and acidified it to pH 1.9 with HCl for an extended time afterward. The Cr(VI) that was left in solution converts to Cr(III) which we then analyze by a second double-spike  $\text{Mg}(\text{OH})_2$  coprecipitation and column purification. Some Cr(VI) isotopic compositions were calculated using the concentration and isotopic composition of total Cr and Cr(III) by mass balance. Additionally, we analyze Cr(III) concentrations and isotope ratios by Cr(III) double-spike isotope dilution either at sea or immediately following thawing of frozen samples. Three samples were processed in both ways and all give the same results (*SI Appendix, Fig. S3*). The method for total Cr concentration and isotopic composition is described in detail in ref. 11. All of our samples have a within-run error of 0.02 to 0.19‰ (2 SE) on  $\delta^{53}\text{Cr}$ . The average [Cr] and  $\delta^{53}\text{Cr}$  values of a long-term in-house seawater standard are  $3.20 \pm 0.12$  nmol/kg (SD,  $n = 20$ ) and  $1.02 \pm 0.13$ ‰ (2 SD,  $n = 20$ ), respectively.

## Results

We analyzed 10 seawater samples for Cr(III) in the ETNP ODZ (100 to 725 m) from cruises RR1805 (April 2018) and KM1920 (September 2019). Although the samples were taken in different seasons, the Cr(III) profiles coincide with no evident seasonal variability (*SI Appendix, Fig. S4*). The concentration of Cr(III) ranges from 0.42 to 1.66 nmol/kg, with the highest concentration observed in the upper ODZ ( $\sim 200$  m; Fig. 3). Cr(III) in this depth range accounts for 11 to 64% of the total dissolved Cr at the same depth. The Cr(III) isotope composition is  $\sim 1$ ‰ lighter than total dissolved Cr ( $\delta^{53}\text{Cr} = 0.93$  to  $1.20$ ‰), ranging from  $\delta^{53}\text{Cr} = -0.14$  to  $0.52$ ‰, with the heaviest isotope signature also seen at 200 m. Total dissolved Cr shows minimal variation in both concentration and isotopic composition in the upper 250 m water column (2.49 to  $\sim 2.87$  nmol/kg and 1.12 to  $\sim 1.24$ ‰, respectively). However, an enrichment in concentration from 2.49 to 5.02 nmol/kg and depletion of heavy  $\delta^{53}\text{Cr}$  from 1.20 to 0.60‰ were observed below 250 m to the bottom (Fig. 4).

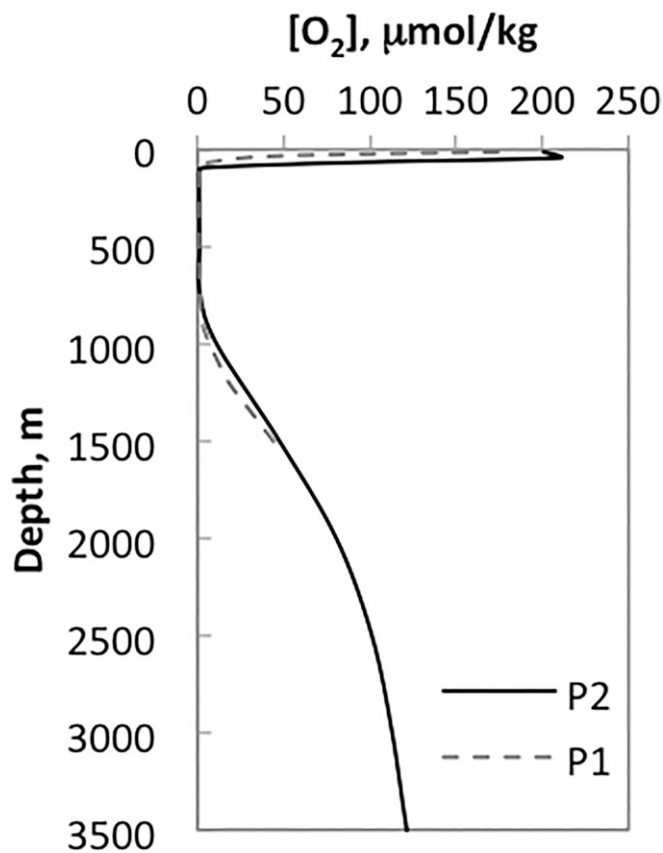


Fig. 2. Dissolved Seabird CTD oxygen profile of stations P1 and P2.

Although oxygen is equally deficient throughout the entire depth range of this ODZ station (90 to 800 m, Fig. 2), both the Cr(III) concentration and  $\delta^{53}\text{Cr}(\text{III})$  peak at 175 to 250 m. This finding is consistent with an early published profile which also shows a [Cr(III)] maximum in the upper ODZ (200 to 300 m) (5). However, our data for [Cr(III)] are 2 to 3 times higher than those reported by Rue et al. (5), who used a different method to selectively extract Cr(III) (solid phase extraction onto Chelex resin). A recently published dataset of Cr species data using the Chelex method in the same region (14) gives a completely different numbers and patterns from Rue et al.'s and ours. The discrepancy between these datasets may result from the different methods we used and the analytical error of the Chelex method. We argue that our data are accurate and more reliable for the

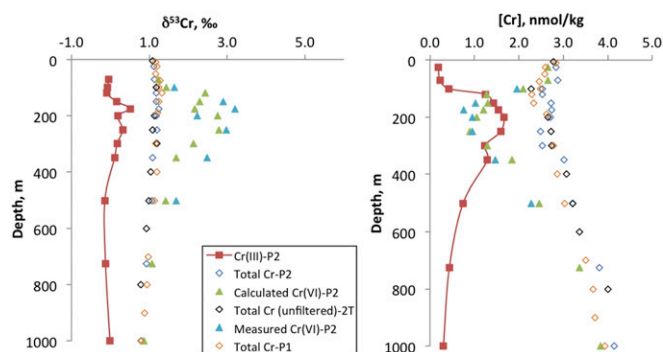


Fig. 3. (Left)  $\delta^{53}\text{Cr}$  and (Right) [Cr] profiles of different dissolved Cr species in the upper 1,000 m of stations P1 and P2.

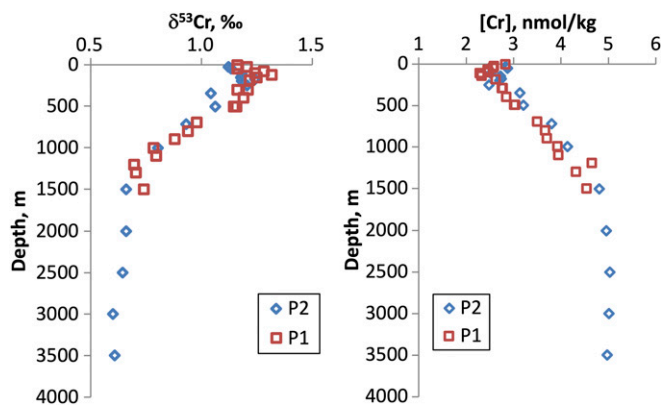


Fig. 4. Full water column profiles of (Left)  $\delta^{53}\text{Cr}$  and (Right)  $[\text{Cr}]$  at stations P1 and P2.

following reasons: 1) Our total Cr concentration data are in line with two other datasets in the ETNP ODZ (5, 21), whereas the total Cr in the surface waters of ref. 14 is too high. 2) A study on  $\text{Mg}(\text{OH})_2$  coprecipitation as a Cr(III) extraction method has demonstrated the robustness of this method (22). 3) We extracted eight Cr(III) samples from the NH1410 cruise by a similar Chelex method (with the resin added to unacidified samples at sea and released from the stored resin later in the laboratory) and found a similar concentration to that reported by Rue et al. (5) (*SI Appendix, Table S2 and Fig. S1*) but lower than reported by ref. 14. Hence, this discrepancy appears to be due to the different Cr(III) extraction methods used by the two studies. One possibility is that the  $\text{Mg}(\text{OH})_2$  precipitation scavenges organic Cr complexes that are thermodynamically stronger than Chelex or have such slow dissociation kinetics that the Cr is inaccessible to binding by Chelex. Establishing the causes of this methodological difference should be a prime target for future research.

Comparing our data to those of a nearby station (NH1410, station 2T) (21) where acidified unfiltered samples (total dissolvable Cr) were collected and analyzed, there is no apparent difference in both Cr concentrations and isotopic compositions between the dissolved (filtered) and the total dissolvable (unfiltered) Cr pools in the upper 800 m water column (Fig. 3). This indicates that the particulate Cr is a small fraction of total Cr, no more than about 5%, which is also consistent with previous reports of particulate Cr concentration (2, 23). This observation is not inconsistent with the observation of scavenging of Cr(III) from the water column. For example, only ~17% of the total  $^{230}\text{Th}$  in seawater is in the particulate form (24), yet Th has a residence time of only about 10 to 40 y in the middle and deep water column due to scavenging (25). Extrapolations of CFC data suggest a water residence time of about 20 y in the upper ETNP ODZ (26), and the occurrence of >50% retained Cr(III) in the ODZ suggests that its residence time is on the order of 50 y. Scaling by analogy to  $^{230}\text{Th}$  (dividing 17% by 50 y/20 y = 6.8%), the scavenging of Cr(III) by a particulate concentration composing ~5% of the total Cr is reasonable.

The Cr isotope and concentration peak appears at 175 to 200 m and is somewhat deeper than the secondary nitrite maximum (~150 m) observed from the same station on this cruise. A similar feature was observed in the same region where nitrogen isotopes showed maximal denitrification at 250 to 300 m (27). The same cooccurrence of slightly lower  $[\text{Cr}]$  with heavier  $\delta^{53}\text{Cr}$  and nitrite accumulation is also observed in the Peruvian ODZ (20). The greater extent of reduction in the upper ranges of the ODZ compared to deeper samples implies that low  $\text{O}_2$  in itself is

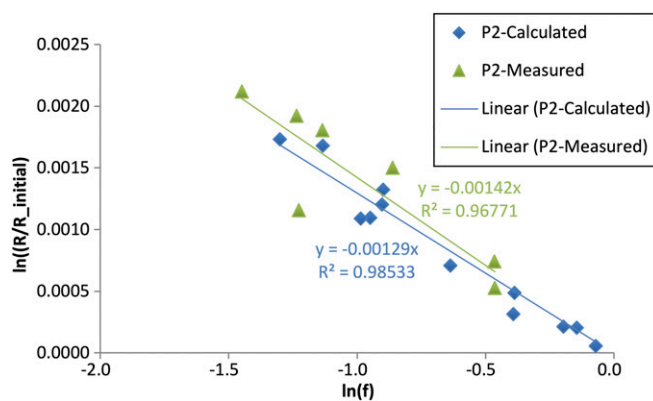


Fig. 5. Progressive closed-system conversion of Cr(VI) to Cr(III) with constant fractionation.

not sufficient for Cr reduction. It seems likely, as seen in the nitrogen system (28, 29), that reduction is dependent on the higher flux of organic matter in the upper water column (30), with the organic matter being used by microbes as the electron donor for the Cr reduction. It would be worthwhile to investigate whether microbial nitrate/nitrite reducers are responsible for Cr reduction in the ODZ (17). Another possible reducing agent for ODZ Cr reduction is Fe(II), as proposed by some studies (20, 21).  $\text{dFe(II)}$  measurement in the ETNP ODZ at a nearby station ( $20^\circ\text{N}$ ,  $107.1^\circ\text{W}$ ) shows accumulation of  $\text{dFe(II)}$  also in the upper core of the ODZ, peaking at 110 m (31). Although  $\text{dFe(II)}$  could reduce Cr(VI) on the timescale of minutes to months in natural environments as shown in experimental studies (32, 33), with limited information, we are not able to pinpoint the mechanism responsible for Cr reduction in the ODZ.

In addition to the analytically determined Cr(VI), Cr(VI) concentrations and isotope compositions also were calculated assuming a mass balance of total dissolved Cr [Cr(III) + Cr(VI)] (Fig. 5 and *SI Appendix, Table S1*). The calculated and measured Cr(VI) data agree with each other considering the relatively large uncertainties from error propagation. The calculated  $[\text{Cr(VI)}]$  ranges from 0.90 to 2.46 nmol/kg from 100 to 500 m. Comparing this with the Cr(III) concentration (Fig. 3 and *SI Appendix, Table S1*), we find that Cr(III) dominates above 300 m in the ODZ while Cr(VI) does so below 300 m. The Cr(VI)

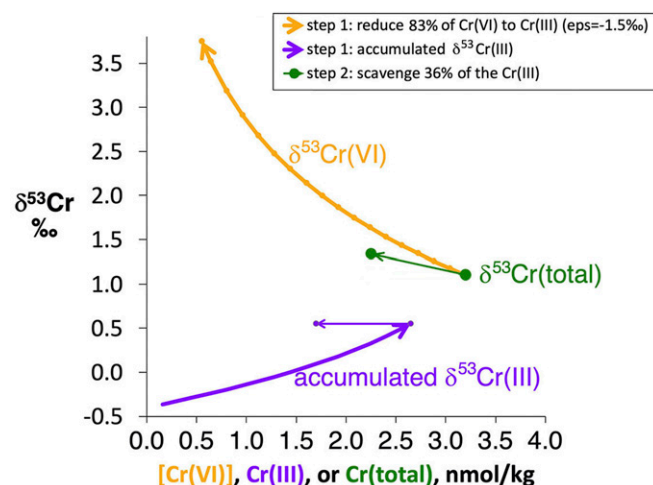


Fig. 6. Stepwise illustration of Cr isotope evolution at the Cr(III) maximum of station P2.



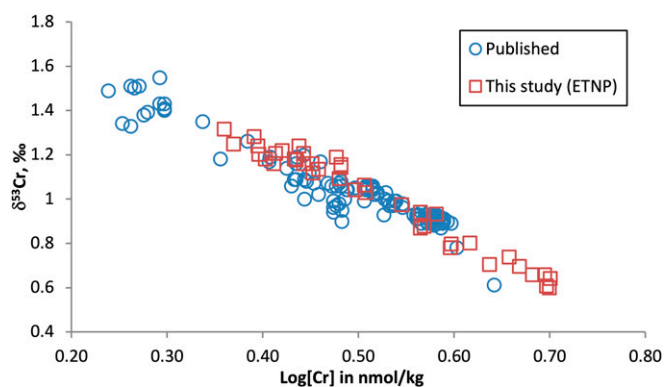


Fig. 7.  $\delta^{53}\text{Cr}$  versus  $\log[\text{Cr}]$  in nmol/kg (10, 11).

isotopic composition is heavier than Cr(III) by 1.5 to 3.1‰. This significant difference between Cr(III) and Cr(VI) isotope compositions supports the mechanism of preferential reduction of light Cr(VI) (16–19).

Previous studies have reported an apparent Rayleigh fractionation factor  $\alpha$  of  $-0.8\text{‰}$  associated with biological uptake/regeneration processes inferred from the global  $\delta^{53}\text{Cr}$  -  $\log[\text{Cr}]$  correlation (10). We calculated the fractionation factor  $\alpha$  for Cr reduction in the ODZ based on the closed-system (Cr(VI) depletion = Cr(VI) initial - Cr(VI) observed) Rayleigh fractionation assumption

$$\frac{R_{\text{sw}}}{R_{\text{sw}}^0} = f^{\alpha-1},$$

where  $R_{\text{sw}}^0$  is the initial  $^{53}\text{Cr}/^{52}\text{Cr}$  of seawater,  $R_{\text{sw}}$  is the ratio of the remaining seawater after reduction,  $f$  is the fraction of Cr remaining in seawater, and  $\alpha$  is the isotopic fractionation factor of Cr reduction. Calculating  $f$  and  $R_{\text{sw}}$  by Cr(III) and  $\sigma_{\theta}$ -adjusted total Cr concentration and isotope values (from the differences between [Cr] and Cr isotopes at the same density at the oxic SAFE station) (21), we determined the fractionation factor in the ODZ to be  $-1.3 \pm 0.1\text{‰}$  (2 SE), which is larger than that inferred from the global (presumed biological)  $\delta^{53}\text{Cr}$ - $\log[\text{Cr}]$  slope ( $-0.8\text{‰}$ ). This difference is real despite the fact that the ODZ total dissolved Cr isotopes fall on the global biogenic relationship. This apparent contradiction can be understood by realizing that a large fraction of the ODZ total dissolved Cr consists of both Cr(III) and Cr(V), with light Cr(III) balancing the heavy Cr(VI), so a significant portion of the total dissolved Cr consists of the light Cr reduced from the residual heavy Cr(VI). ODZ [Cr] and light Cr isotope depletion occurs because only a fraction of the generated light Cr(III) is removed onto sinking particles. Fig. 6 illustrates this pathway for the ODZ Cr(III) maximum:  $\sim 83\%$  of the Cr(VI) in seawater entering the ODZ from the oxic ocean is converted to Cr(III) (with a presumed constant isotope fractionation) that makes the Cr(VI) progressively heavier along a Rayleigh fractionation path. Isotopically light Cr(III) accumulates and becomes slightly heavier as the source Cr(VI) evolves. Although there may be a small isotopic fractionation associated with scavenging, we have no evidence for this and hence assume that dissolved and scavenged Cr(III) have identical isotopic compositions. Only a moderate fraction ( $\sim 36\%$ ) of the generated Cr(III) is scavenged by sinking particles, leaving behind significant dissolved Cr(III). The end result depends on the fraction of the original Cr(VI) that is reduced and the fraction of Cr(III) scavenged.

A previous study on Si isotope systematics (34) points out that a linear correlation between logarithmic concentration and isotopic composition does not necessarily translate to a single fractionation process but may involve a composite of processes (surface uptake, regeneration, thermocline ventilation, and ocean mixing and circulation). A similar argument of Cr isotope systematics was proposed in ref. 20 that the global apparent fractionation factor, which is also applicable to ODZ dataset, represents a net effect of reduction and scavenging in the ODZ. We corroborate this statement here by arguing that the fractionation factor we determined ( $-1.3 \pm 0.1\text{‰}$ ) reflects the Cr(VI) reduction process in the ODZ. However, the one determined from the global  $\delta^{53}\text{Cr}$ - $\log[\text{Cr}]$  plot reflects a complex signal arising from reduction and surface biological uptake, followed by scavenging and regeneration in the deep ocean. The fact that our data fall on the global Cr array indicates that Cr cycling in the ETNP ODZ is in line with the global Cr cycling despite the unique reduction process. It is not evident why the extent of reduction and the fraction of Cr(III) remaining in the water column result in a total dissolved  $\delta^{53}\text{Cr}$ - $\log[\text{Cr}]$  pathway matching the oxic ocean biological removal and regeneration relationship (Fig. 7). We therefore ascribe this observation to a coincidence that might not occur in oceans with different conditions. It requires further investigation into the origin of the global Cr array, which is not the scope of this study but is critical in understanding global Cr cycling. However, our dataset can help identify some of the processes governing the global Cr distribution. For instance, a previous study (30) has observed a particle maximum in the ETNP ODZ at the same depth where we observe maximum Cr reduction and removal, and this factor may interplay with the reduction and scavenging processes.

## Conclusions

Concentration and isotope analyses of Cr(III) and Cr(VI) confirm the reduction of hexavalent Cr [Cr(VI)] to trivalent Cr [Cr(III)] followed by partial scavenging of Cr(III) in the ETNP ODZ. Cr(III) is  $\sim 2\text{‰}$  lighter than the residual Cr(VI) in the ODZ, showing the preferential reduction of isotopically light Cr. The Cr(III) concentration maximum appears in the upper core of the ODZ, near the nitrate  $^{15}\text{N}$  isotope maximum and secondary nitrite maximum, which implies microbially mediated Cr reduction. The fractionation factor of Cr reduction determined by calculated Cr(VI) isotope ratios assuming closed-system Rayleigh fractionation is  $-1.3 \pm 0.1\text{‰}$ . This fractionation factor is greater than that determined by the global  $\delta^{53}\text{Cr}$ - $\log[\text{Cr}]$  plot, which can be explained by the partial removal of the reduced Cr(III). The fact that the total dissolved Cr data of this study fall on the global  $\delta^{53}\text{Cr}$ - $\log[\text{Cr}]$  line is attributed to a coincidence dependent on many factors (particle fluxes, etc.). Further worthwhile investigation could be directed at the mechanisms of Cr reduction in the ODZ by examining potential reducing agents including dissolved Fe(II) and denitrifiers.

**Data Availability.** All study data are included in the article, *SI Appendix*, and *Dataset S1*.

**ACKNOWLEDGMENTS.** We thank chief scientist Gabrielle Rocap for accommodating us on cruises *Roger Revelle* 1804-5 and *Kilo Moana* 19-20 (sponsored by NSF Grant DEB-1542240 to G. Rocap, A. Devol, R. Kiel, and C. Deutch), Jim Moffett for helping with sampling on these cruises, and Mark Altabet and Frank Stewart for collecting the samples from station 2T on cruise *New Horizon* 1410. We also thank the officers and crews of these ships for their efforts on our behalf. Rick Kayser helped with laboratory maintenance. We thank reviewers Chris Holmden and Sam Jaccard for their constructive comments. This research was supported by NSF Grant OCE-1736996 (to E.A.B.) and by a fellowship from the Massachusetts Institute of Technology/Woods Hole Oceanographic Institution Joint Program in Oceanography.

1. C. Jeandel, J. F. Minster, Chromium behavior in the ocean: Global versus regional processes. *Global Biogeochem. Cycles* **1**, 131–154 (1987).
2. R. E. Cranston, J. W. Murray, The determination of chromium species in natural waters. *Anal. Chim. Acta* **99**, 275–282 (1978).
3. R. E. Cranston, J. W. Murray, Chromium species in the Columbia River and estuary. *Limnol. Oceanogr.* **25**, 1104–1112 (1980).
4. R. J. Kieber, G. R. Helz, Indirect photoreduction of aqueous chromium (VI). *Environ. Sci. Technol.* **26**, 307–312 (1992).
5. E. L. Rue, G. J. Smith, G. A. Cutter, K. W. Bruland, The response of trace element redox couples to suboxic conditions in the water column. *Deep Sea Res. Part I Oceanogr. Res. Pap.* **44**, 113–134 (1997).
6. L. Stramma, G. C. Johnson, J. Sprintall, V. Mohrholz, Expanding oxygen-minimum zones in the tropical oceans. *Science* **320**, 655–658 (2008).
7. G. Shaffer, S. M. Olsen, J. O. P. Pedersen, Long-term ocean oxygen depletion in response to carbon dioxide emissions from fossil fuels. *Nat. Geosci.* **2**, 105–109 (2009).
8. S. O. Schlanger, H. C. Jenkyns, Cretaceous oceanic anoxic events: Causes and consequences. *Neth. J. Geosci.* **55**, 3–4 (1976).
9. S. P. Hesselbo *et al.*; Morgans Bell HS, Massive dissociation of gas hydrate during a Jurassic oceanic anoxic event. *Nature* **406**, 392–395 (2000).
10. L. J. Janssen, M. Amini, C. Holmden, R. Francois, Global variability of chromium isotopes in seawater demonstrated by Pacific, Atlantic, and Arctic Ocean samples. *Earth Planet. Sci. Lett.* **423**, 87–97 (2015).
11. S. B. Moos, E. A. Boyle, Determination of accurate and precise chromium isotope ratios in seawater samples by MC-ICP-MS illustrated by analysis of SAFe Station in the North Pacific Ocean. *Chem. Geol.* **511**, 481–493 (2019).
12. D. J. Janssen *et al.*, Biological control of chromium redox and stable isotope composition in the surface ocean. *Global Biogeochem. Cycles* **34**, e2019GB006397 (2020).
13. J. Rickli, D. J. Janssen, C. Hassler, M. J. Ellwood, S. L. Jaccard, Chromium biogeochemistry and stable isotope distribution in the Southern Ocean. *Geochim. Cosmochim. Acta* **262**, 188–206 (2019).
14. X. Wang, J. B. Glass, C. T. Reinhard, N. J. Planavsky, Species-dependent chromium isotope fractionation across the Eastern Tropical North Pacific oxygen minimum zone. *Geochim. Geophys. Geosyst.* **20**, 2499–2514 (2019).
15. E. Schauble, G. R. Rossman, H. P. Taylor Jr., Theoretical estimates of equilibrium chromium isotope fractionations. *Chem. Geol.* **205**, 99–114 (2004).
16. L. N. Døssing, K. Dideriksen, S. L. S. Stipp, R. Frei, Reduction of hexavalent chromium by ferrous iron: A process of chromium isotope fractionation and its relevance to natural environments. *Chem. Geol.* **285**, 157–166 (2011).
17. E. R. Sikora, T. M. Johnson, T. D. Bullen, Microbial mass-dependent fractionation of chromium isotopes. *Geochim. Cosmochim. Acta* **72**, 3631–3641 (2008).
18. J. W. Kitchen, T. M. Johnson, T. D. Bullen, J. Zhu, A. Raddatz, Chromium isotope fractionation factors for reduction of Cr (VI) by aqueous Fe (II) and organic molecules. *Geochim. Cosmochim. Acta* **89**, 190–201 (2012).
19. A. S. Ellis, T. M. Johnson, T. D. Bullen, Chromium isotopes and the fate of hexavalent chromium in the environment. *Science* **295**, 2060–2062 (2002).
20. P. Nasemann *et al.*, Chromium reduction and associated stable isotope fractionation restricted to anoxic shelf waters in the Peruvian oxygen minimum zone. *Geochim. Cosmochim. Acta* **285**, 207–224 (2020).
21. S. B. Moos, E. A. Boyle, M. A. Altabet, A. Bourbonnais, Investigating the cycling of chromium in the oxygen deficient waters of the Eastern Tropical North Pacific Ocean and the Santa Barbara Basin using stable isotopes. *Mar. Chem.* **221**, 103756 (2020).
22. A. B. Davidson *et al.*, Mg(OH)<sub>2</sub> coprecipitation method for determining chromium speciation and isotopic composition in seawater. *Limnol. Oceanogr. Methods* **18**, 8–19 (2020).
23. J. W. Murray, B. Spell, B. Paul, “The contrasting geochemistry of manganese and chromium in the eastern tropical Pacific Ocean” in *Trace Metals in Sea Water*, C. S. Wong, E. Boyle, K. W. Bruland, J. D. Burton, E. D. Goldberg, Eds. (Springer, 1983), pp. 643–669.
24. M. P. Bacon, R. F. Anderson, Distribution of thorium isotopes between dissolved and particulate forms in the deep sea. *J. Geophys. Res.* **87**, 2045–2056 (1982).
25. G. M. Henderson, R. F. Anderson, “The U-series toolbox for paleoceanography” in *Uranium-Series Geochemistry*, B. Bourdon, G. M. Henderson, C. C. Lundstrom, S. P. Turner, Eds. (De Gruyter, 2003), vol. 52, pp. 493–531.
26. R. M. Fine, K. A. Maillet, K. F. Sullivan, D. Willey, Circulation and ventilation flux of the Pacific Ocean. *J. Geophys. Res.* **106**, 22159–22178 (2001).
27. C. A. Fuchsman *et al.*, An N isotopic mass balance of the Eastern Tropical North Pacific oxygen deficient zone. *Deep Sea Res. Part II Top. Stud. Oceanogr.* **156**, 137–147 (2018).
28. B. A. Van Mooy, R. G. Keil, A. H. Devol, Impact of suboxia on sinking particulate organic carbon: Enhanced carbon flux and preferential degradation of amino acids via denitrification. *Geochim. Cosmochim. Acta* **66**, 457–465 (2002).
29. D. Bianchi, T. S. Weber, R. Kiko, C. Deutsch, Global niche of marine anaerobic metabolisms expanded by particle microenvironments. *Nat. Geosci.* **11**, 263–268 (2018).
30. P. C. Garfield, T. T. Packard, G. E. Friederich, L. A. Codispoti, A subsurface particle maximum layer and enhanced microbial activity in the secondary nitrite maximum of the northeastern tropical Pacific Ocean. *J. Mar. Res.* **41**, 747–768 (1983).
31. K. M. Bolster, M. I. Heller, J. W. Moffett, Determination of iron (II) by chemiluminescence using masking ligands to distinguish interferences. *Limnol. Oceanogr. Methods* **16**, 750–759 (2018).
32. D. L. Sedlak, P. G. Chan, Reduction of hexavalent chromium by ferrous iron. *Geochim. Cosmochim. Acta* **61**, 2185–2192 (1997).
33. M. Pettine, L. D’ottone, L. Campanella, F. J. Millero, R. Passino, The reduction of chromium (VI) by iron (II) in aqueous solutions. *Geochim. Cosmochim. Acta* **62**, 1509–1519 (1998).
34. D. Reynolds, M. Frank, A. N. Halliday, Silicon isotope fractionation during nutrient utilization in the North Pacific. *Earth Planet. Sci. Lett.* **244**, 431–443 (2006).